CRYSTAL GROWTH & DESIGN

Article

pubs.acs.org/crystal

Crystal Inclusion Formation of a New Type of Dumbbell-Shaped Host Compound Featuring Two Bulky 2,3,4,5-Tetraphenylcyclopenta-2,4-dien-1-ol Terminal Groups Attached to a Linear Spacer Unit

Alexander Ruffani, Wilhelm Seichter, Anke Schwarzer, and Edwin Weber*

Institut für Organische Chemie, Technische Universität Bergakademie Freiberg, Leipziger Strasse 29, D-09596 Freiberg, Sachsen, Germany

Supporting Information

ABSTRACT: Four new host compounds of dumbbell shape featuring bulky 2,3,4,5-tetraphenylcyclopenta-2,4-dien-1-ol moieties attached to both ends of a linear spacer element of different lengths comprising both 1,4-phenylene and ethynylene subunits are synthesized and corresponding crystal inclusions involving DMSO, DMF, MeCN, and THF as guest solvents (seven examples of inclusion compounds) are isolated. X-ray structural analysis shows the formation of 1:2 host/guest entities being a basic supramolecular motif of the crystal inclusions. Nevertheless, additional solvent molecules seem to be necessary for stabilization of the crystal structure in most cases of the inclusion species indicating the occurrence of unusually high stoichiometric ratios of included solvent as a specific characteristic of the new type of host molecule.

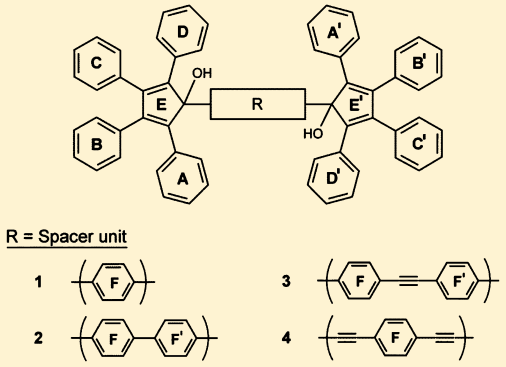

INTRODUCTION

The crystal engineering of solid-state materials is of ever-increasing interest to chemists and materials scientist alike.[1−4] Selective formation of crystal inclusion compounds is one of the main challenges in this area of research.[5−7] This has given rise to the design of a variety of host compounds, all being intended to entrap molecular guests in their crystal lattice.[8,9] A guiding principle which has proven very successful in this respect involves the presence of a rather bulky and rigid molecular construction, in order to prevent close packing, and also inside located polar, mainly hydrogen donor/acceptor groups, allowing for specific guest interaction.[10] This concept is commonly referred to as the "coordinato-clathrate" approach.[11] Representative examples of host structures developed from this line of thought correspond to wheel-and-axle,[12,13] scissor-like,[14] roof-shaped,[11] or dumbbell type[15−17] molecular geometries.

The host compounds presented in this paper belong to the latter subclass of compounds, i.e., the dumbbell type, but are new in their respective constitutions. In particular, they contain a 2,3,4,5-tetraphenylcyclopenta-2,4-dien-1-ol moiety, which is an especially bulky group, attached to the ends of a linear spacer element differing in length. As a result of this specific structural feature, crystal inclusion compounds are formed that attract attention due to the remarkably high content of guest solvent, in some cases besides some other structural characteristics, reported in this paper. In a more detailed specification, we describe the synthesis of the dumbbell-shaped host compounds **1**−**4**, including seven examples of corresponding solvent inclusions (Scheme 1) and discuss the X-ray crystal structures of the inclusion complexes. A few known, in a way related, host compounds[18,19] containing the same bulky 2,3,4,5-tetraphenylcyclopenta-2,4-dien-1-ol moiety, but as a monofunctional species showing a more simple molecular constitution, are worth mentioning at this point and will be regarded in the discussion.

RESULTS AND DISCUSSION

Host Synthesis. The host compounds **1**−**4** (Scheme 1) were synthesized from tetracyclone and the respective organyldilithium compound, the latter being prepared from the respective aryl dibromide (1,4-dibromobenzene, 4,4′-dibromobiphenyl, 4,4′-dibromotolane) or 1,4-diethynylbenzene and *n*-BuLi, following a method described for the preparation of **1** and **2**.[20] The tetracyclone was obtained from benzil and 1,3-diphenylpropan-2-one according to the established procedure.[21] 4,4′-Dibromotolane was synthesized from bibenzyl via a bromination and elimination route,[22,23] while 1,4-dibromobenzene is commercially available. 1,4-Diethynylbenzene was prepared by Pd-catalyzed cross-coupling reaction[24] of 1,4-dibromobenzene with 2-methylbut-3-yn-2-ol,[25] and subsequent cleavage of the blocking group.[26] Because of the high affinity of the host compounds to retain solvent molecules, attainment of satisfactory elemental analyses caused difficulties. Moreover, in the ^{13}C NMR spectrum of compound **3**, the carbon signal for the symmetric acetylene group is not clearly perceptible. However,

Received: March 9, 2016
Revised: April 28, 2016

DOI: 10.1021/acs.cgd.6b00383
Cryst. Growth Des. XXXX, XXX, XXX−XXX

Scheme 1. Chemical Formula Structures Including Ring Specification of the Studied Host Molecules 1−4 and Specification of Corresponding Inclusion Compounds

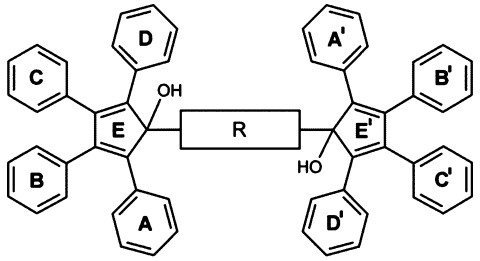

R = Spacer unit

1 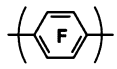

2 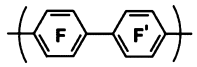

3 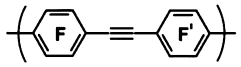

4 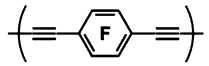

1a = **1** · DMSO (1:3)
1b = **1** · DMF (1:4)
2a = **2** · CH_3CN (1:1)
2b = **2** · DMF (1:3)
2c = **2** · THF (1:6)
3a = **3** · DMSO (1:2)
4a = **4** · DMSO (1:5)

the Raman spectrum for this compound indicated a definite band for the carbon triple bond at 2220 cm^{-1}.

X-ray Structural Study of Inclusion Compounds. The hosts **1**−**4** yielded crystalline inclusion compounds with a selection of mainly polar guest solvents. They involve DMSO and DMF, both being of strong polar aprotic nature, and as exceptions of this particular solvent class acetonitrile and THF being aprotic solvents of weaker polarity, giving rise to a variety of corresponding crystalline inclusions (**1a**, **1b**, **2a**−**2c**, **3a**, and **4a**) specified in Scheme 1. Not only because of the unusual host/guest stoichiometry showing a remarkably high guest ratio from 1:3 to 1:6, in some of the cases, considering the bifunctionality of the host molecules, but also because of the newness of the host constitutions in general, crystal structures of the present inclusion compounds are to be expected to offer interesting insight into the inclusion behavior of these specific host molecules. However, it should already be noted at this point that **4a** (**4**·DMSO, 1:5) raised difficulties to obtain perfect crystals for X-ray diffraction. For all inclusion compounds, crystallographic data and refinement parameters are presented in Table 1, while geometric parameters and information regarding hydrogen bonding in the crystals are summarized in Tables 2 and 3, respectively. Perspective views of the molecular structures including selected atom numbering and specification of ring units are shown in Figure 1 (a complete numbering system of atoms is given in Figure S1). Illustrations of the packing structures inclusive of excerpts of relevant interaction modes are displayed in Figure 2, Figure 3, Figure 4, Figure 5, and Figure 6 offering properties as stated in the following.

In the inclusion structures formed of **1**−**4**, the phenyl rings within the pentacyclic end groups of the host molecules exhibit a propeller-like arrangement around the cyclopentadiene ring which reduces intramolecular sterical strain. Consequently, restricted conformational freedom is found within these units as deducible from the geometric parameters listed in Table 2. The conformational features of the diol hosts may be described best by calculation of interplanar angles which define the inclination of the phenyl rings with respect to the plane of the cyclopentadiene ring to which they are attached. In order to simplify the characterization of the crystal structures, the ring fragments of the molecules are marked by capital letters in Scheme 1 and in the figures showing the molecular structures.

Crystallization of **1** from dimethyl sulfoxide yields colorless plates of **1a** crystallizing in the orthorhombic space group $Pna2_1$ with the asymmetric part of the unit cell containing one host molecule and three molecules of solvent (Figure 1a). Taking into account experimental error, the double bonds within the cyclopentadiene rings have identical bond lengths [1.350(3)−1.353(3) Å]. Because of conjugation effects, the $C(sp^2)$−$C(sp^2)$ single bonds within these rings are significantly shorter [1.497(3), 1.499(3) Å] than the $C(sp^2)$−$C(sp^3)$ single bonds [1.510(3)−1.536(3) Å]. The lengths of $C(sp^2)$−C(arene) single bonds range between 1.474(4) and 1.490(3) Å, $C(sp^3)$−C(arene) bonds are 1.536(3) [1.539(3) Å]. These values are comparable to those found in the crystal structure of 1,2,3,4,5-pentaphenylcyclopenta-2,4-dien-1-ol,[18] which represents the basic building unit of the diol hosts discussed in this paper. The central aromatic ring F is oriented nearly orthogonal with respect to the cyclopentadiene rings [87.8(1), 89.7(1)°]. According to their distinctive acceptor character two of the guest molecules are linked to the host via conventional hydrogen bonds, whereas an only weak C−H···O contact[27] is formed by the third highly disordered guest molecule. The crystal packing of **1a** (Figure 2a) reveals layers of host and guest molecules being stacked in alternating order in direction of the crystallographic *c*-axis. The aromatic nature of the host molecules give rise to extensive intermolecular association via C−H···π arene hydrogen bonds.[28] It should be mentioned that in this type of interactions individual carbon atoms of aromatic rings instead of commonly used ring centroids were chosen as acceptor positions to obtain well-defined hydrogen bond geometries (see Table 3). The H···C distances of these contacts range between 2.69 and 2.87 Å, which is shorter than the sum of the van der Waals radii of carbon and hydrogen (2.90 Å). Within a given layer of guest molecules, the molecular dipoles are aligned along the *a*-axis.

Similar structural features are also found in the inclusion compound of **1** with dimethylformamide (1:4) **1b**, although the host−guest stoichiometric ratio differs from that of **1a**. The asymmetric entity of the unit cell (space group $P\bar{1}$) contains one-half of the diol host and two guest molecules; i.e., the host molecule adopts inversion symmetry which implies an *anti*-configuration of its hydroxy groups. An ORTEP diagram of the molecular structure is depicted in Figure 1b. As can be seen from the structure motif in Figure 3, one fraction of guest molecules forms the expected O−H···O hydrogen bonds to the host, whereas the remaining guest molecules are involved in relatively short C−H_{arene}···O contacts. Moreover, C−H···O hydrogen bond interactions connect the guest molecules to one another. According to the given mode of hydrogen bonding, host and guest molecules are connected to supramolecular layers extending parallel to the crystallographic *ac* plane. At first sight, the packing of molecules in **1a** (Figure 2a) and of the present

DOI: 10.1021/acs.cgd.6b00383
Cryst. Growth Des. XXXX, XXX, XXX−XXX

Table 1. Crystallographic Data and Structure Refinement Details of the Compounds Studied

	1a	1b	2a	2b	2c	3a	4a
empirical formula	$C_{64}H_{46}O_2 \cdot 3\ C_2H_6SO$	$C_{64}H_{46}O_2 \cdot 4\ C_3H_7NO$	$C_{70}H_{50}O_2 \cdot C_2H_3N$	$C_{70}H_{50}O_2 \cdot 3\ C_3H_7NO$	$C_{70}H_{50}O_2 \cdot 6\ C_4H_8O$	$C_{72}H_{50}O_2 \cdot 2\ C_2H_6SO$	$C_{68}H_{46}O_2 \cdot 5\ C_2H_6SO$
formula weight	1081.39	1139.39	964.15	1142.39	1355.72	1103.38	1285.68
crystal system	orthorhombic	triclinic	monoclinic	orthorhombic	triclinic	triclinic	triclinic
space group	$Pna2_1$	$P\bar{1}$	$P2_1/n$	$Pna2_1$	$P\bar{1}$	$P\bar{1}$	$P\bar{1}$
a (Å)	19.3505(9)	10.7086(19)	12.1097(13)	19.2031(17)	12.5805(4)	10.1911(5)	11.433(3)
b (Å)	12.2201(6)	11.723(2)	15.663(2)	11.5414(11)	12.9715(4)	14.6772(6)	17.248(4)
c (Å)	23.9692(11)	14.007(3)	14.7211(19)	28.503(3)	25.0354(7)	19.9043(9)	18.017(5)
α (deg)	90.0	109.664(9)	90.0	90.0	87.870(2)	91.830(3)	102.515(11)
β (deg)	90.0	97.625(9)	106.422(4)	90.0	79.883(2)	92.067(2)	98.379(12)
γ (deg)	90.0	105.381(9)	90.0	90.0	64.200(2)	94.945(2)	92.969(10)
V (Å^3)	5667.9(5)	1548.1(5)	2678.4(6)	6317.1(10)	3617.5(2)	2962.4(2)	3418.7(15)
Z	4	1	2	4	2	2	2
$F(000)$	2288	606	1016	2424	1452	1164	1360
D_c (Mg m^{-3})	1.267	1.222	1.196	1.201	1.245	1.237	1.249
μ (mm^{-1})	0.184	0.077	0.071	0.074	0.078	0.142	0.224
data collection							
temperature (K)	93(2)	153(2)	93(2)	123(2)	93(2)	93(2)	93(2)
no. of collected reflections	60450	25652	21893	109789	41325	44672	55013
within the θ-limit (deg)	2.1−28.4	1.6−27.5	2.3−25.1	1.9−26.5	1.9−27.1	1.7−25.0	1.17−25.0
index ranges $\pm h, \pm k, \pm l$	−25/25, −16/14, −32/31	−13/13, −15/13, −18/18	−14/8, −18/18, −16/17	−24/23, −14/14, −35/35	−16/16, −16/16, −32/29	−12/12, −17/17, −23/23	−13/13, −20/20, −21/21
no. of unique reflections	14198	7006	4642	12981	15640	10149	11725
R_{int}	0.0949	0.0629	0.1041	0.1436	0.0301	0.1087	0.0747
refinement calculations: full-matrix least- squares on all F^2 values							
weighting expression w[a]	$[\sigma^2(F_0^2) + (0.0339P)^2 + 0.7712P)^{-1}$	$[\sigma^2(F_0^2) + (0.0657P)^2 + 0.6022P)^{-1}$	$[\sigma^2(F_0^2) + (0.0453P)^2 + 1.9124P)^{-1}$	$[\sigma^2(F_0^2) + (0.0475P)^2 + 0.0000P)^{-1}$	$[\sigma^2(F_0^2) + (0.0664P)^2 + 0.8439P)^{-1}$	$[\sigma^2(F_0^2) + (0.0754P)^2 + 0.8525P)^{-1}$	$[\sigma^2(F_0^2) + (0.1343P)^2 + 47.3024P)^{-1}$
no. of refined parameters	718	393	343	793	921	753	817
no. of F values used $[I > 2\sigma(I)]$	8579	3676	2415	7615	10977	4792	8435
final R-Indices							
$R(=\Sigma\lvert\Delta F\rvert/\Sigma\lvert F_0\rvert)$	0.0476	0.0554	0.0542	0.0457	0.0512	0.0607	0.1667
wR on F^2	0.0942	0.1669	0.1463	0.1054	0.1415	0.1633	0.4215
S (= goodness of fit on F^2)	0.839	1.012	1.004	0.884	1.104	0.875	1.154
final $\Delta\rho_{max}/\Delta\rho_{min}$ (e·Å^{-3})	0.57/-0.34	0.41/-0.24	0.28/-0.33	0.42/-0.40	0.45/-0.24	0.57/-0.34	1.20/-0.86

[a] $P = (F_0^2 + 2F_c^2)/3$.

DOI: 10.1021/acs.cgd.6b00383
Cryst. Growth Des. XXXX, XXX, XXX−XXX

Table 2. Selected Conformational Parameters and Bond Lengths in the Crystal Structures of 1a,b, 2a−c, 3a, and 4a

compound	1a	1b	2a	2b	2c	3a	4a
			Dihedral Angles (deg)				
mpla(A)/mpla(E)	51.4(1)	42.9(1)	34.6(1)	51.6(1)	36.1(1)	33.1(2)	47.6(4)
mpla(B)/mpla(E)	40.0(1)	50.9(1)	57.1(1)	47.6(1)	41.5(1)	51.7(1)	52.7(3)
mpla(C)/mpla(E)	44.4(1)	37.1(1)	54.2(1)	56.0(1)	58.9(1)	51.9(1)	47.6(3)
mpla(D)/mpla(E)	81.5(1)	54.7(1)	55.6(1)	47.0(1)	57.6(1)	60.6(1)	55.1(3)
mpla(E)/mpla(F)	87.8(1)	85.3(1)	87.3(1)	84.7(1)	87.4(1)	89.6(1)	86.4(3)
mpla(A′)/(E′)	39.4(1)			79.7(1)	40.8(1)	32.7(2)	32.0(5)
mpla(B′)/(E′)	50.0(1)			57.1(2)	46.6(1)	55.4(1)	55.2(3)
mpla(C′)/(E′)	40.5(1)			47.6(1)	59.8(1)	59.2(1)	48.8(3)
mpla(D′)/(E′)	69.5(1)			45.8(1)	64.5(1)	35.4(1)	75.9(3)
mpla(E′)/(F)	89.7(1)			89.9(1)	80.6(1)		83.4(3)
mpla(F)/(F′)				10.7(2)	18.2(1)	16.8(1)	
mpla(E′)/(F′)						86.3(1)	
			Torsion Angles (deg)				
C(30)−C(1)−O(1)−H(1)	−170.5(1)		69.9(1)	−175.0(1)	−172.8(1)	−173.1(1)	42.5(5)
C(33)−C(36)−O(2)−H(2)	171.6(1)						
C(39)−C(1)−O(1)−H(1)		−176.0(1)					
C(39)−C(40)−O(2)−H(2)							−39.5(5)
C(39)−C(42)−O(2)−H(2)				171.6(1)	175.9(1)		
C(41)−C(44)−O(2)−H(2)						91.0(1)	91.0(1)
bond lengths (Å)							
C(1)−C(2)	1.510(3)	1.530(3)	1.531(3)	1.527(5)	1.540(2)	1.524(5)	1.543(12)
C(2)−C(3)	1.353(3)	1.354(3)	1.352(4)	1.345(5)	1.350(2)	1.362(5)	1.337(12)
C(3)−C(4)	1.499(3)	1.509(3)	1.499(4)	1.497(5)	1.498(2)	1.493(5)	1.508(11)
C(4)−C(5)	1.352(3)	1.344(3)	1.353(4)	1.347(5)	1.340(2)	1.345(5)	1.336(12)
C(1)−C(5)	1.527(4)	1.538(3)	1.526(4)	1.530(5)	1.530(2)	1.546(5)	1.559(12)
C(1)−C(30)	1.536(3)	1.529(3)	1.520(4)	1.528(5)	1.530(2)	1.529(5)	1.498(12)
C(33)−C(36)						1.442(6)	
C(36)−C(37)		1.524(3)					
C(37)−C(38)		1.351(3)				1.439(6)	
C(38)−C(39)		1.497(4)					
C(39)−C(40)		1.350(3)					1.485(11)
C(36)−C(40)		1.536(4)					
C(33)−C(36)		1.539(3)					
C(41)−C(44)						1.542(5)	
C(42)−C(43)				1.531(5)	1.533(2)		
C(43)−C(44)				1.350(5)	1.342(2)		
C(44)−C(45)				1.494(5)	1.495(2)	1.529(5)	
C(45)−C(46)				1.345(5)	1.349(2)	1.359(5)	
C(46)−C(47)						1.484(5)	
C(47)−C(48)						1.348(5)	
C(48)−C(44)						1.524(5)	
C(42)−C(46)				1.532(5)	1.539(2)		
C(39)−C(42)				1.522(5)	1.530(2)		

structure (Figure 2b) appear similar, showing layers of host and guest molecules being stacked in an alternating order. The occurrence of different space group symmetries, however, implies structural differences. While in the crystal structure of **1a**, the orientation of host molecules of consecutive layers are related by the 2-fold screw axis; in the structure of **1b** the inversion symmetry of the host molecule results in a unique orientation of the molecules.

Crystals of the diol **2** obtained from CH_3CN turned out to be an inclusion compound (**2a**) of the host/guest ratio of 1:1 with the guest molecule CH_3CN disordered around the symmetry center. This means that only one OH group of the host molecule acts as a donor for hydrogen bonding. The stoichiometric unit of **2a** is displayed in Figure 1c. The central phenyl rings of the host are not perfectly planar giving rise to the molecule to adopt a slight S-shaped bend along its biphenyl spacer moiety. The packing diagram of **2a** (Figure 4a) reveals that the crystal is composed of 1:1 host−guest complexes being linked via C−H···O bonding to infinite chains extending parallel to the crystallographic *c*-axis. Interconnection between supramolecular chains is realized by C−H···π-interactions between the aromatic rings.

The inclusion compound of **2** with dimethylformamide (1:3) (**2b**) crystallizes in the orthorhombic space group $Pna2_1$ ($Z = 4$); i.e. the host molecule lacks a center of inversion. The twist angle between the rings of the central biphenyl unit is 10.7(2)°. As expected, two of the guest molecules contribute to formation of 1:2 host−guest units via O−H···O hydrogen bonding (Figure 1d). The remaining solvent molecule is involved in guest−guest association with its oxygen atom acting as a bifurcated acceptor. In the crystal lattice, the host molecules are packed in such a manner as to leave channels running along the

DOI: 10.1021/acs.cgd.6b00383
Cryst. Growth Des. XXXX, XXX, XXX−XXX

Table 3. Selected Noncovalent Interactions in the Inclusion Structures of 1a,b, 2a−c, 3a, and 4a

atoms involved D−H···A	symmetry	distance D···A	H···A	angle, D−H···A
1a				
O(1)−H(1)···O(1F)	−*x*, 1−*y*, 0.5+*z*	2.867(3)	2.04	167.7
O(2)−H(2)···O(1G)	1+*x*, *y*, 1+*z*	2.773(3)	1.94	173.1
C(29)−H(29)···O(1F)	1−*x*, 1−*y*, 0.5+*z*	3.527(3)	2.67	150.4
C(64)−H(64)···O(1G)	1+*x*, *y*, 1+*z*	3.562(4)	2.69	153.2
C(1F)−H(1F3)···O(2)	−0.5+*x*, 1.5−*y*, −1+*z*	3.380(4)	2.66	130.3
C(57)−H(57)···O(1H)	1+*x*, −1+*y*, 1+*z*	3.613(4)	2.72	157.1
C(48)−H(48)···C(20)[a]	0.5+*x*, 1.5−*y*, *z*	3.709(4)	2.77	168.1
C(20)−H(20)···C(42)[a]	−0.5+*x*, 1.5-*y*, *z*	3.529(4)	2.70	145.5
C(13)−H(13)···C(55)[a]	−0.5+*x*, 0.5−*y*, *z*	3.714(4)	2.81	159.7
C(28)−H(28)···C(57)[a]	2−*x*, 1−*y*, −0.5+*z*	3.678(4)	2.80	157.9
1b				
O(1)−H(1)···O(1G)	*x*, *y*, *z*	2.746(3)	1.91	171.0
C(7)−H(7)···O(1)	*x*, *y*, *z*	3.109(4)	2.46	125.5
C(3H)−H(3H3)···O(1G)	1+*x*, *y*, *z*	3.482(5)	2.61	148.7
C(14)−H(14)···O(1H)	1−*x*, 2−*y*, 1−*z*	3.195(3)	2.48	131.6
C(3G)−H(3G1)···O(1)	−*x*, 2−*y*,1−*z*	3.667(3)	2.69	175.7
C(2G)−H(2G3)···O(1H)	*x*, *y*, *z*	3.440(5)	2.52	156.4
C(8)−H(8)···C(27)[a]	*x*, 1+*y*, *z*	3.758(4)	2.85	160.4
2a				
O(1)−H(1)···N(1A)	*x*, −1+*y*, *z*	3.055(5)	2.25	160.4
C(13)−H(13)···O(1)	1−*x*, −*y*, 1−*z*	3.438(6)	2.52	161.4
C(7)−H(7)···O(1)	*x*, *y*, *z*	3.080(6)	2.41	127.3
C(17)−H(17)···C(9)[a]	1.5−*x*, 0.5+*y*, 1.5−*z*	3.699(6)	2.80	158.8
C(2)−H(21)···C(15)[a]	1−*x*, 1−*y*, 1−*z*	3.697(6)	2.81	156.8
2b				
O(1)−H(1)···O(1H)	*x*, *y*, *z*	2.623(4)	1.81	161.7
O(2)−H(2)···O(1F)	−1+*x*, *y*, *z*	2.686(4)	1.85	176.3
C(2H)−H(2H1)···O(1G)	0.5+*x*, 0.5−*y*, *z*	3.477(10)	2.61	147.1
C(2F)−H(2F1)···O(1G)	1−*x*, 1−*y*, 0.5+*z*	3.453(7)	2.68	136.4
C(3H)−H(3H3)···O(2)	0.5−*x*, −0.5+*y*, −0.5+*z*	3.408(8)	2.67	132.3
C(2G)−H(2G3)···C(11)[a]	*x*, −1+*y*, *z*	3.614(8)	2.76	146.8
C(8)−H(8)···C(64)[a]	0.5+*x*, 2.5−*y*, *z*	3.640(7)	2.80	147.5
C(10)−H(10)···C(21)[a]	*x*, 1+*y*, *z*	3.725(8)	2.79	167.7
C(41)−H(41)···C(10)[a]	−0.5+*x*, 2.5−*y*, *z*	3.539(8)	2.72	144.2
C(69)−H(69)···C(13)[a]	−0.5+*x*, 1.5−*y*, *z*	3.623(7)	2.83	141.8
2c				
O(1)−H(1)···O(1H)	−*x*, 2−*y*, 1−*z*	2.774(2)	1.94	171.1
O(2)−H(2)···O(1F)	1−*x*, 1−*y*, −*z*	2.787(2)	1.96	170.2
C(11)−H(11)···O(1)	*x*, *y*, *z*	3.087(2)	2.41	127.9
C(52)−H(52)···O(2)	*x*, *y*, *z*	3.140(2)	2.49	125.3
C(49)−H(49)···O(1G)	*x*, *y*, *z*	3.447(2)	2.59	150.3
C(56)−H(56)···O(1J)	*x*, −1+*y*, *z*	3.548(3)	2.76	140.8
C(57)−H(57)···O(1I)	*x*, −1+*y*, *z*	3.455(3)	2.71	135.3
C(16)−H(16)···O(1K)	−1+*x*, 1+*y*, *z*	3.545(3)	2.74	142.8
C(1G)−H(1G1)···*Cg*(B)[b]	1+*x*, *y*, *z*	3.571(4)	2.67	151.9
C(3H)−H(3H2)···*Cg*(D)[b]	*x*, −1+*y*, *z*	3.761(4)	2.83	157.3
3a				
O(1)−H(1)···O(1G)	*x*, *y*, 1+*z*	2.820(4)	1.98	173.3
O(2)−H(2)···O(1H)	*x*, *y*, *z*	2.717(4)	2.01	141.4
C(1G)−H(1G3)···O(1H)	1+*x*, *y*, *z*	3.332(5)	2.41	156.7
C(7)−H(7)···O(1)	*x*, *y*, *z*	3.054(5)	2.38	128.0
C(8)−H(8)···O(1G)	2−*x*, 1−*y*, 1−*z*	3.329(5)	2.51	144.8
C(72)−H(72)···O(2)	*x*, *y*, *z*	2.981(5)	2.31	126.8
C(28)−H(28)···*Cg*(B)[b]	−1+*x*, *y*, *z*	3.508(5)	2.62	156.0
C(53)−H(53)···*Cg*(D)[b]	*x*, *y*, −1+*z*	3.723(5)	2.84	155.1
C(66)−H(66)···C(52)[a]	−1+*x*, *y*, *z*	3.448(5)	2.65	142.2
C(1G)−H(1G1)···C(13)[a]	*x*, *y*, −1+*z*	3.633(5)	2.70	159.7
4a				
O(1)−H(1)···O(1C)	−*x*, 1−*y*, 1−*z*	2.701(13)	1.91	154.9
O(2)−H(2)···O(1B)	*x*, *y*, *z*	2.690(10)	1.88	162.9

DOI: 10.1021/acs.cgd.6b00383
Cryst. Growth Des. XXXX, XXX, XXX−XXX

Table 3. continued

atoms involved D−H···A	symmetry	distance D···A	H···A	angle, D−H···A
C(1A)−H(1A1)···O(1)	1+*x*, −1+*y*, *z*	3.319(18)	2.51	140.5
C(1A)−H(1A3)···O(1D)	*x*, *y*, −1+*z*	3.160(18)	2.25	156.5
C(2B)−H(2B2)···O(1E)	−1+*x*, *y*, *z*	3.377(18)	2.52	142.7
C(1C)−H(1C2)···O(1A)	*x*, *y*, 1+*z*	3.420(20)	2.60	142.4
C(1C)−H(1C3)···O(1B)	*x*, *y*, 1+*z*	3.477(18)	2.59	151.5
C(2C)−H(2C2)···O(1A)	*x*, *y*, 1+*z*	3.252(20)	2.37	145.8
C(29)−H(29)···O(1)	*x*, *y*, *z*	3.053(14)	2.51	116.3
C(1E)−H(1E3)···O(2)	*x*, *y*, *z*	3.381(20)	2.50	152.1
C(34)−H(34)···O(1E)	1−*x*, 1−*y*, −*z*	3.128(12)	2.34	139.5
C(66)−H(66)···O(1D)	−1+*x*, *y*, −1+*z*	3.211(20)	2.49	132.8

[a]To obtain a reasonable hydrogen bond geometry, an individual atom of an aromatic ring instead of the ring center was chosen as an acceptor. [b]*Cg* means the center of an aromatic ring. **2c**, **3a**: Ring B: C(6)···C(11) ; ring D: C(18)···C(23).

crystallographic *a*-axis with the hydroxy groups sticking out of the hydrophobic channel walls. Within a given channel, the guest molecules form infinite C−H···O bonded strands with a unique alignment of their dipoles (Figure 4b). Compared with **1b**, the elongation of the host axis by an additional phenyl group markedly influences the mode of host−host interaction leading to formation of multiple C−H···π arene contacts [d(H···π) 2.72−2.83 Å].

Replacement of a highly coordinating dipolar aprotic guest solvent (DMF) by a less polar guest species has a fundamental influence on the host lattice structure which is evident from the inclusion compound of **2** with tetrahydrofuran **2c** versus **2b**. In the crystal structure of **2c** (space group $P\bar{1}$), the content of the asymmetric part of the unit cell, which is shown in Figure 1e, has the very unusual host/guest stoichiometric ratio of 1:6. Two of the guest molecules are linked in the expected way to the host molecule by conventional O−H···O hydrogen bonds, while the remaining guests participate in weak C−H···O contacts to host arene hydrogens, but are not cross-linked among each other. A view of the crystal structure along the *a*-axis (Figure 5a) reveals a complex arrangement consisting of layers of guest molecules which extend along the *ab*-plane and such guests being incorporated in channel-like lattice voids of an irregular cross-section with a maximum extension of 13.6 × 3.7 Å. Thus, a remarkable feature of the inclusion structure is that 40.7% of the crystal volume is occupied by solvent molecules. This high content of crystal solvent may also explain the relatively poor cross-linking of the host molecules.

Crystallization of **3** from DMSO yields a 1:2 solvent inclusion compound **3a** with the asymmetric part of the unit cell containing one host molecule and two molecules of DMSO, one of them disordered over two positions (s.o.f. 0.86, 0.14) (Figure 1f). The host molecule shows a slight bend along the diphenylethyne spacer moiety and a dihedral angle of 16.8(1)° with reference to the aromatic rings (F,F′). These rings are arranged nearly orthogonal [89.6(1), 86.3(1)°] with respect to the planes of the cyclopentadienyl rings. The overall geometry of the host molecule basically differs from those of **1** and **2**, showing a *syn* orientation of the hydroxy groups. In the crystal of **3a**, the guest molecules are connected via O−H···O hydrogen bonding to the host molecule leading to 1:2 complex units as basic supramolecular entities. They are packed in such a way that the pentacyclic moieties of the host molecules fit into the cleft left by the narrow spacer of an adjacent molecule (Figure 5b) thus allowing a closely packed structure. Host−host interaction is accomplished by C−H···O hydrogen bonding and by a number of C−H···π arene contacts leading to a three-dimensional network. Pairs of guest molecules reside in closed lattice voids created by aromatic rings of six host molecules.

As already indicated at the beginning, multiple attempts of growing crystals of **4** from DMSO permanently gave only crystals (**4a**) of poor quality leading to a data set of low resolution ($\theta_{max} \approx 22.0°$). Nevertheless, we succeeded to solve the crystal structure which, however, could not be refined to an acceptable level. This is evident from a high *R*-value. The number of observed reflections represents less than 50% of the number of unique reflections. Taking into account the conditions, the crystals were found to belong to the space group $P\bar{1}$ with the asymmetric part of the unit cell comprising one host molecule and five molecules of DMSO, two of them disordered over two positions. A perspective view of the molecular structure is displayed in Figure 1g. Because of packing forces, the 1,4-diethynylphenylene spacer of the host molecule slightly deviates from linearity. The aromatic ring of this unit is inclined at angles of 83.0(2) and 86.1(2)° with respect to the planes of the cyclopentadiene rings. The 3D architecture of this inclusion compound exhibits similarities with **1a** and **1b**, showing a layered arrangement of host and guest molecules. An excerpt of the packing structure of **4a** is shown in Figure 6a. The high extent of crystal solvent induces the formation of different supramolecular entities. As displayed in Figure 6b, one of the host hydroxyl groups and two of the solvent molecules contribute to the formation of infinite double strand-like supramolecular aggregates comprising host−guest O−H···O and C−H···O as well as guest−guest C−H···O interactions. The pattern of hydrogen bonding within a strand can be regarded as being composed of fused cyclic synthons[2] following the graph sets $R_6^4(16)$ and $R_4^4(18)$.[29] The second host hydroxyl group and the remaining solvent molecules are connected via hydrogen bonds of the O−H···O and C−H···O type to give a cyclic structure aggregate (Figure 6c). The central supramolecular motif of this unit is represented by the graph set $R_6^6(20)$.

CONCLUSION

The attachment of bulky 2,3,4,5-tetraphenylcyclopenta-2,4-dien-1-ol moieties to both ends of a linear spacer element of different length comprising both 1,4-phenylene and ethynylene subunits has proven to be a structural host design for the formation of crystalline solvent inclusions. As a matter of principle, this should be explained to the effect that the high sterical shielding of the host functional groups by the bulk of the pentacyclic building blocks prevents self-aggregation of the host molecules via conventional hydrogen bonding. Therefore, a

DOI: 10.1021/acs.cgd.6b00383
Cryst. Growth Des. XXXX, XXX, XXX−XXX

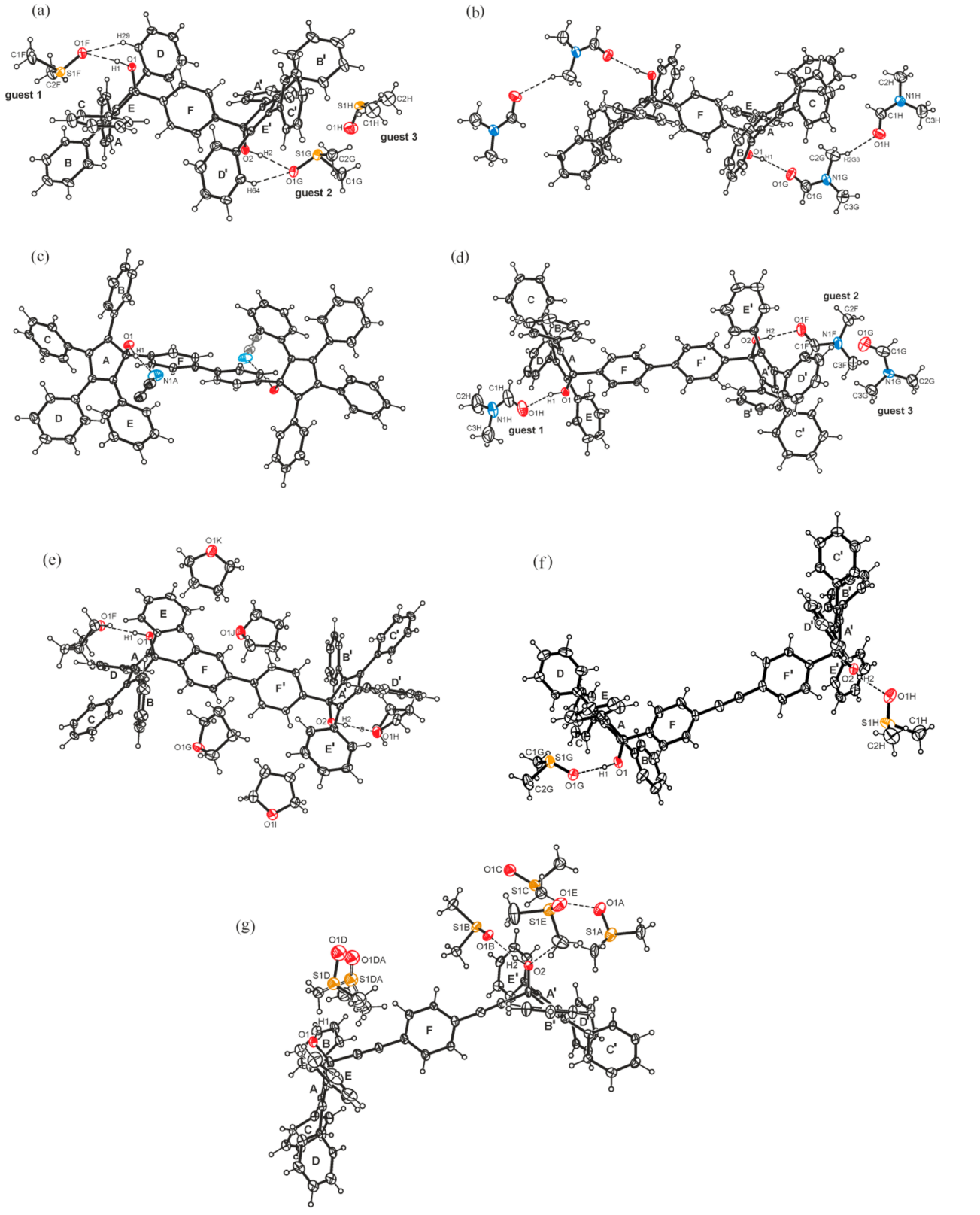

Figure 1. Molecular structures (ORTEP plots with 50% probability level) of the inclusion compounds **1a** (a), **1b** (b), **2a** (c), **2b** (d), **2c** (e), **3a** (f), and **4a** (g) involving numbering of relevant atoms and specification of ring units (A–F). Complete numbering systems of atoms and ring specifications of the host molecules are given in Figure S1. In panel c, the two disorder positions of the solvent molecule are indicated in bold and light style.

secondary coordinating species of appropriate size (solvent molecule) is an essential prerequisite for the formation of an inclusion crystal corresponding with the basic idea of the coordinato-clathrate strategy,[11] while the general structure of the molecules **1**–**4** meets the dumbbell shape construction principle[15−17] also favoring inclusion formation. Thus, both the

DOI: 10.1021/acs.cgd.6b00383
Cryst. Growth Des. XXXX, XXX, XXX−XXX

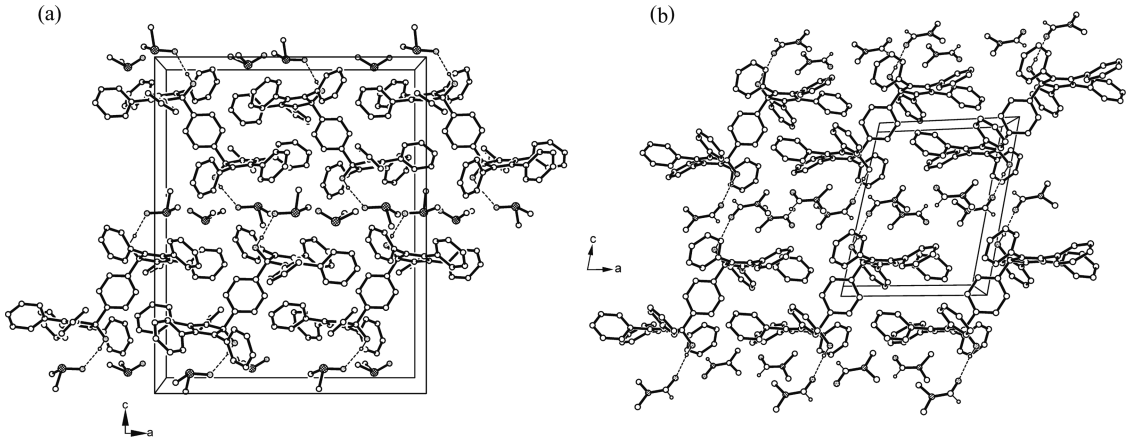

Figure 2. Packing diagrams of **1a** (a) and **1b** (b). Oxygens are displayed as dotted, nitrogens as hatched and sulfur atoms as cross-hatched circles. Nonrelevant hydrogen atoms have been omitted for the sake of clarity. Dashed lines represent hydrogen bond interactions.

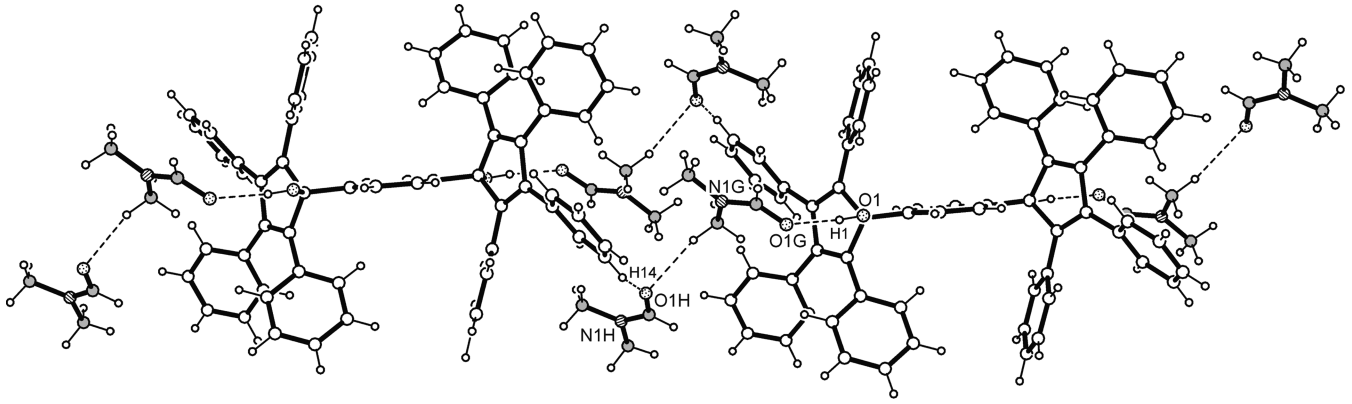

Figure 3. Packing excerpt showing the strand formation of host and guest molecules in the structure of **1b**. Dashed lines represent hydrogen bond interactions.

hydrophobic nature of the host framework and the presence of a polar guest species determine the three-dimensional molecular assembly in the inclusion crystals formed of **1**−**4**. Being connected with this feature, it seems that the aggregation of the host molecules is strongly driven by the formation of an optimal number of arene−arene contacts with edge-to-face geometry which is restricted to the accessible aromatic rings of the end groups but leaving those of the spacer elements uneffected. Moreover, with the exception of **2a**, a common feature is the formation of 1:2 host/guest units that represent the basic supramolecular entities of the crystal structures in parallel with the bifunctionality of the host molecules.

Nevertheless, despite these things in common, distinct differences in the structure of the respective inclusion crystals can be observed. While only in the case of **3a** the 1:2, respectively, in **2a** the 1:1 host−guest units enable effective packing in the crystal, in all the other structures the formation of a close packing requires additional solvent molecules. They involve host/guest stoichiometric ratios ranging from 1:3 (**1a**, **2b**) via 1:4 (**1b**) and 1:5 (**4a**) to the unusually high host:guest ratio of 1:6 in **2c**, showing up to four additional solvent molecule, respectively, for the stabilization of the crystal packing. Hence, the ability for storage of high ratios of solvent in the crystal structure of inclusion compounds in some cases is a salient feature of the compound class. At constant bulkiness of the terminal groups, this is likely to be related to the length of the spacer element, but this is difficult to put in concrete terms. At any rate, a change in length of the spacer element of the host obviously influences the packing behavior as schematized in Figure 7. That is to say, the crystal structures of **1a**, **1b**, and **4a** are characterized by a typical layer arrangement of host and guest molecules being stacked in an alternating fashion. The host−guest stoichiometric ratios of 1:3, 1:4, and 1:5 of these structures, respectively, indicate that different patterns of noncovalent bonding within the layers of guest molecules are present. The donor−acceptor behavior of the included solvent in the crystal structure of **2a** leads to formation of discrete O−H···N bonded host−guest aggregates; i.e., no layer formation is observed in this structure. Here, the host molecules of adjacent complexes interact via C−H···π bonding. Compared with **1b**, the elongation of the spacer element by an additional phenyl group induces a channel-like cavity structure, in which the solvent molecules are accommodated. Surprisingly, crystallization of **2** from THF leads to a 1:6 solvate **2c** with the solvent molecules incorporated in channels of the host lattice showing different dimensions and cross sections. Crystal formation of the diols **3** and **4** containing a diphenylethynyl and diethynylphenyl unit as a spacer element, respectively, yields inclusion structures with a *cisoid* arrangement of the pentacyclic terminal moieties, instead of *transoid* as for **1** and **2**, giving the molecules a bowl-like overall geometry. This is also a reason to see that the combination of bulky terminal groups and a narrow well-dimensioned spacer element enables interlocking

DOI: 10.1021/acs.cgd.6b00383
Cryst. Growth Des. XXXX, XXX, XXX−XXX

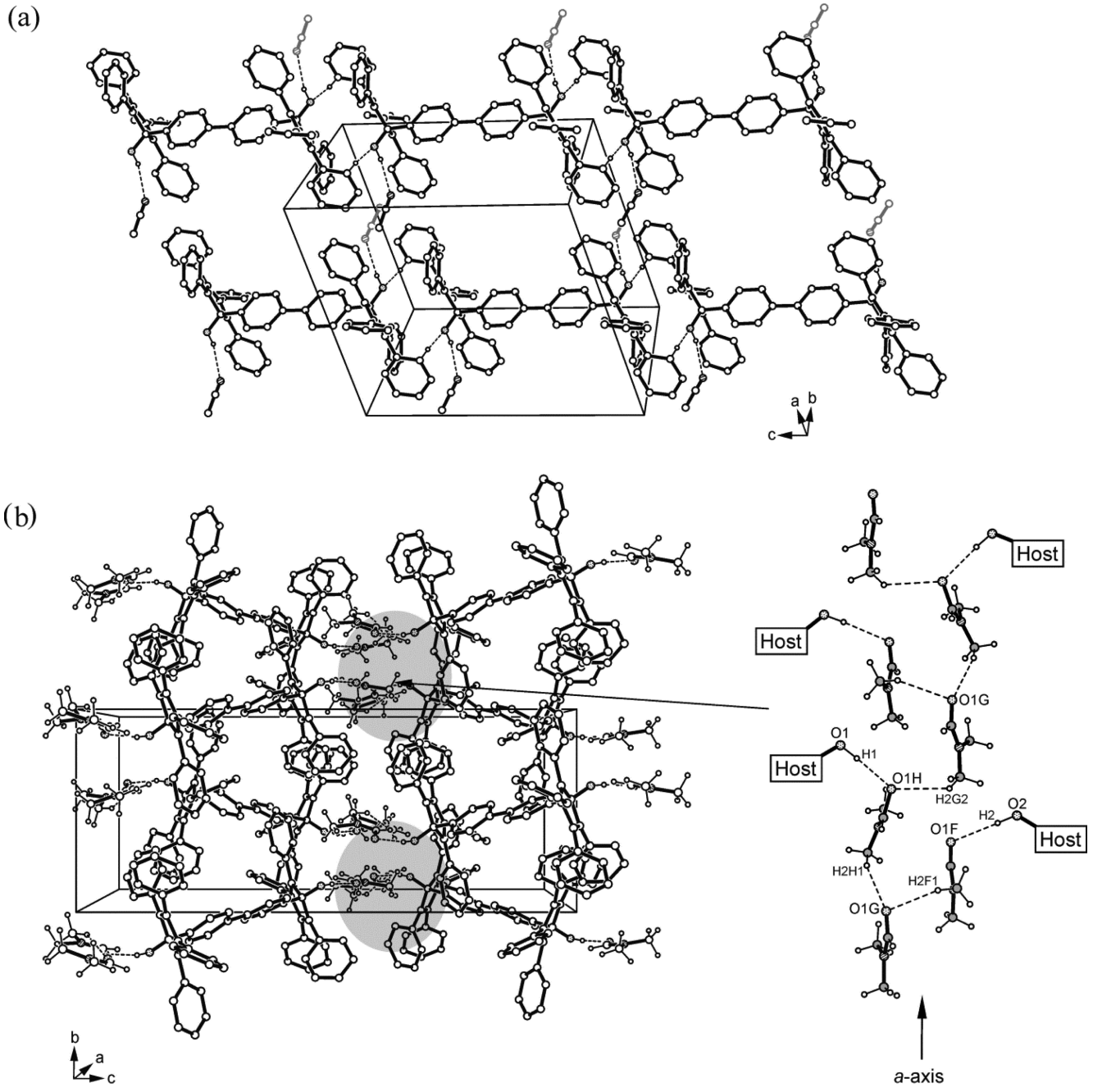

Figure 4. Packing diagrams of **2a** (a) and **2b** (b) including the specific hydrogen bond motif formed in the structure of **2b** (indicated as shaded area). Oxygens are displayed as dotted and nitrogen atoms as hatched circles. Nonrelevant hydrogen atoms have been omitted for the sake of clarity. In panel a, the two disorder positions of the solvent molecule are indicated in bold and light style.

of the molecules to form a closed packing structure with the solvent molecules either accommodated in closed lattice voids (**3a**) or creating a layer structure (**4a**).

In summary, compared to the known solvent inclusion of 1-aryl substituted 2,3,4,5-tetraphenylcyclopentadien-1-ols being simple monofunctional analogues,[18,19] the present structurally extended dumbbell-shaped host molecules **1**−**4** not only give rise to a more diversified inclusion property but also to unusually high stoichiometric ratios of the solvent included in the majority of isolated crystals as a specific feature. This in particular is likely to be beneficial for future host design aiming at the storage[7,30] or the sensing[13,31] of solvents by means of crystalline materials.

EXPERIMENTAL SECTION

General. Melting points are uncorrected. IR spectra were obtained using a Nicolet 510A spectrometer. The Raman spectrum was performed with a Bruker RFS 100/S spectrometer. ^{1}H and ^{13}C NMR spectra were recorded on a Bruker DPX 400 at 25 °C. Chemical shifts are reported in ppm with TMS as an internal standard (δ = ppm). Mass spectra were determined on Bruker ESQUIRE-LC 00084 (ESI) and MICROMASS ZABSPEC (FAB) instruments. The solvents used were purified or dried according to common literature procedures.[32]

Starting Compounds. Tetracyclone,[21] 4,4′-dibromotolane,[22,23] and 1,4-diethynylbenzene[25] were prepared according to published procedures. 1,4-Dibromobenzene and 4,4′-dibromobiphenyl were purchased from Aldrich.

DOI: 10.1021/acs.cgd.6b00383
Cryst. Growth Des. XXXX, XXX, XXX−XXX

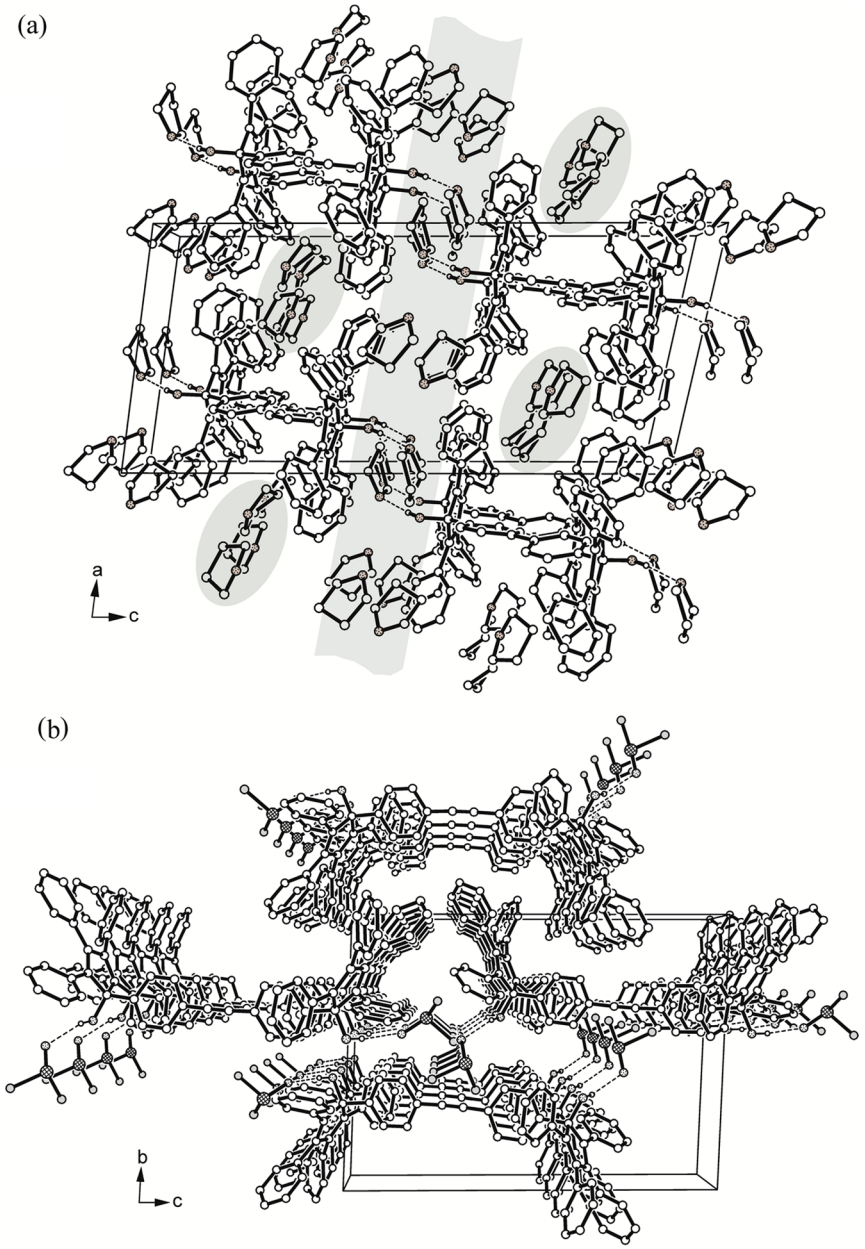

Figure 5. Packing diagrams of **2c** (a) and **3a** (b). Layer and channel-type areas in the packing structure of **2c** are marked by shading. Oxygen atoms are displayed as dotted and sulfur atoms as cross-hatched circles. Dashed lines represent hydrogen bond interactions.

Synthesis of Host Compounds 1−4. General Procedure. [20] Tetracyclone (5.76 g, 15 mmol) was added (at the beginning in portions as a solid and after that as a solution in dry toluene) to a stirred solution of the corresponding organyldilithium compound (8.65 mmol), prepared from the respective aryl dibromide or 1,4-diethynylbenzene (8.65 mmol), at room temperature under argon. Stirring of the mixture was continued until completion of the reaction which is indicated by bleaching of the black-violet color of the tetracyclone. The mixture was then quenched with water and acidified (diluted hydrochloric acid). The organic layer was separated, filtered, and dried (Na_2SO_4). Evaporation of the solvent and extraction with refluxing toluene, in order to remove impurities, yielded the compounds as powders. Details for the individual compounds are given below.

1,1′-(1,4-Phenylene)bis(2,3,4,5-tetraphenylcyclopenta-2,4-dien-1-ol) (1). 1,4-Phenylenedilithium (from 1,4-dibromobenzene and *n*-BuLi) was used to yield 2.19 g (30%) colorless powder. Mp 290 °C (lit.[20] 290−291 °C). IR (KBr, cm^{-1}) 3550 (OH), 3079, 3053, 3028 (Ar−H), 1641, 1600, 1497 (C═C, Ar), 1440, 1078 (C−O), 798, 741, 700. ^{1}H NMR (400 MHz, [D_6]DMSO) δ 6.10 (2H, s, OH), 6.82−7.13 (40H, m, phenyl-H), 7.39 (4H, s, phenylene-H). ^{13}C NMR (100.6 MHz, [D_6]DMSO) δ 89.4 (C−OH), 124.9−148.8 (C═C, Ar). MS (ESI) *m*/*z* Calcd for $C_{64}H_{46}O_2$: 847.1. Found: 847.2.

1,1′-(Biphenyl-4,4-diyl)bis(2,3,4,5-tetraphenylcyclopenta-2,4-dien-1-ol) (2). Biphenyl-4,4′-diyldilithium (from 1,4-dibromobiphenyl and *n*-BuLi) was used to yield 6.56 g (82%) colorless powder. Mp 278 °C (lit.[20] 278−280 °C). IR (KBr, cm^{-1}) 3545 (OH), 3079, 3059, 3028 (Ar−H), 1631, 1605, 1491 (C═C, Ar), 1440, 1078 (C−O), 803, 746, 700. ^{1}H NMR (400 MHz, [D_6]DMSO) δ 5.84 (2H, s, OH), 6.96−7.16 (40H, m, phenyl-H), 7.42 (4H, d, $^3J_{HH}$ = 7.2 Hz, phenylene-H), 7.62 (4H, d, $^3J_{HH}$ = 7.2 Hz, phenylene-H). ^{13}C NMR (100.6 MHz, [D_6]DMSO) δ 88.4 (C−OH), 124.5−147.4 (C═C, Ar). MS (ESI) *m*/*z* Calcd for $C_{70}H_{50}O_2$: 923.2. Found: 923.3.

1,1′-(Ethynylene-di-4,1-phenylene)bis(2,3,4,5-tetraphenylcyclopenta-2,4-dien-1-ol) (3). Ethynylene-di-4,1-phenylenedilithium (from 4,4′-dibromotolane and *n*-BuLi) was used to yield 6.9 g (84%) colorless powder. Mp 290 °C. IR (KBr, cm^{-1}) 3534 (OH), 3084, 3059, 3022 (Ar−H), 1631, 1605, 1491 (C═C, Ar),

DOI: 10.1021/acs.cgd.6b00383
Cryst. Growth Des. XXXX, XXX, XXX−XXX

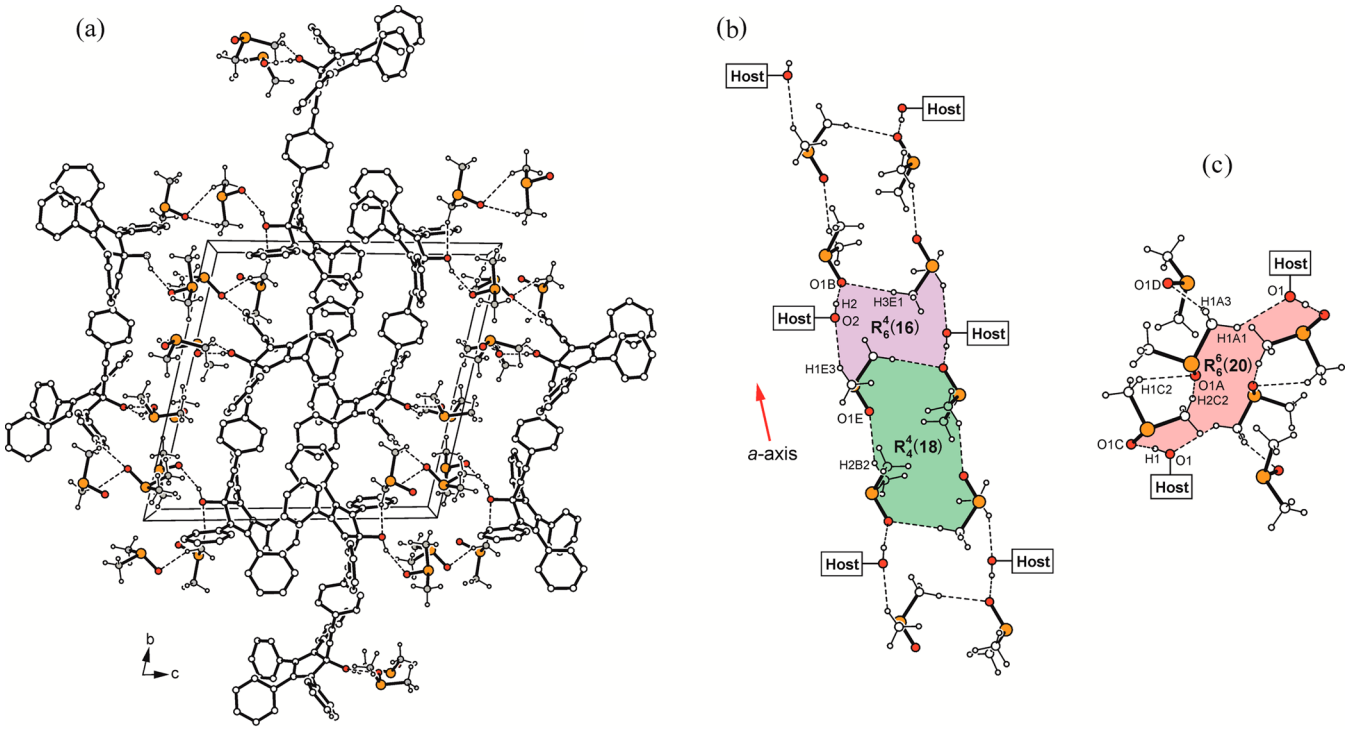

Figure 6. (a) Illustration of the packing structure of **4a** viewed along the crystallographic *a*-axis. Oxygen atoms are displayed as red, sulfur atoms as orange circles. (b) Double strand-like supramolecular structure motif in **4a** with coloring of the cyclic patterns of hydrogen bonding. (c) Supramolecular interaction motif in the crystal structure of **4a**.

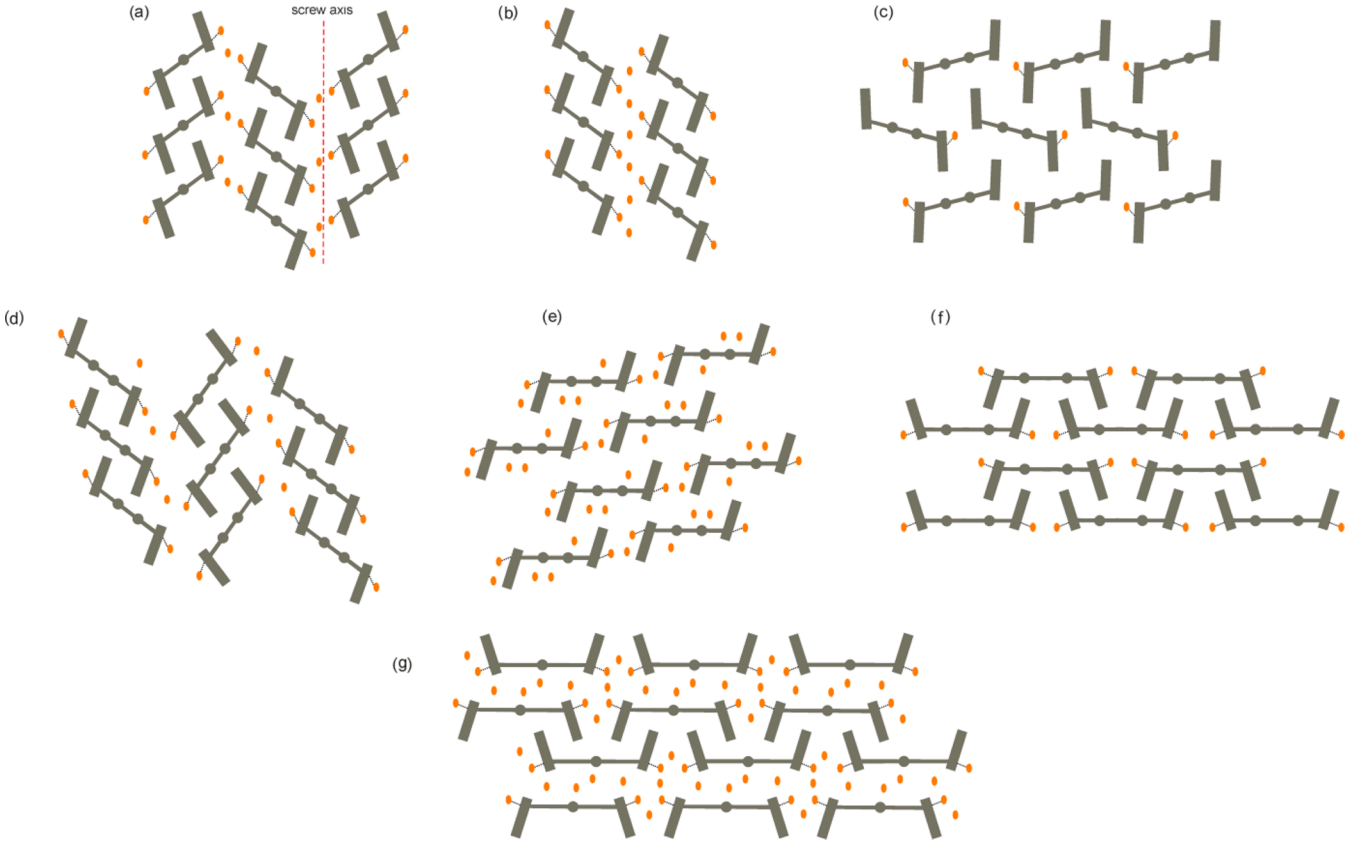

Figure 7. Packing modes of the host molecules in the inclusion structures of **1a** (a), **1b** (b), **2a** (c), **2b** (d), **2c** (e), **3a** (f), and **4a** (g). Guest molecules are displayed as orange ellipses.

DOI: 10.1021/acs.cgd.6b00383
Cryst. Growth Des. XXXX, XXX, XXX−XXX

1440, 1078 (C−O), 803, 747, 705. Raman (neat powder, cm^{-1}) 2220 (C≡C). ^1H NMR (400 MHz, [D_6]DMSO) δ 6.46 (2H, s, OH), 6.96−7.27 (40H, m, phenyl-H), 7.40 (4H, d, $^3J_{HH}$ = 8.4 Hz, phenylene-H), 7.54 (4H, d, $^3J_{HH}$ = 8.4 Hz, phenylene-H). ^{13}C NMR (100.6 MHz, [D_6]DMSO) δ 89.3 (C−OH), 120.4 (*C*-C≡C), 125.4−148.3 (C=C, Ar). MS (ESI) *m*/*z* Calcd for $C_{72}H_{50}O_2$: 947.2. Found: 947.3.

1,1′-(1,4-Phenylene-diethynylene)bis(2,3,4,5-tetraphenylcyclopenta-2,4-dien-1-ol) (4). 1,4-Pheny-lene-diethynylenedilithium (from 1,4-diethynylbenzene and *n*-BuLi) was used to yield 2.65 g (34%) yellow powder. Mp 237 °C. IR (KBr, cm^{-1}) 3529 (OH), 3084, 3053, 3022 (Ar−H), 2221, 2195 (C≡C), 1631, 1610, 1496, 1488 (C=C, Ar), 1445, 1072 (C−O), 804, 700. ^1H NMR (400 MHz, [D_6]DMSO) δ 6.42 (2H, s, OH), 6.90−7.25 (40H, m, phenyl-H), 7.47 (4H, d, phenylene-H). ^{13}C NMR (100.6 MHz, [D_6]DMSO) δ 81.1 (C≡C), 82.9 (C≡C), 92.4 (C−OH), 122.3 (*C*-C≡C), 125.3−143.9 (C=C, Ar). MS (FAB) *m*/*z* Calcd for $C_{68}H_{46}O_2$: 895.1. Found: 895.

Preparation of Inclusion Compounds. Crystals of the inclusion compounds **1a**, **1b**, **2a**−**2c**, **3a**, and **4a** were obtained by slow crystallization from solutions of the respective host compound in the corresponding solvent or slow cooling the respective solutions followed by slow evaporation of solutions if necessary.

X-ray Crystallography. The intensity data of the compounds were collected on a Kappa APEX II diffractometer (Bruker AXS) with MoK_α radiation (λ = 0.71073 Å). Reflections were corrected for background, Lorentz and polarization effects. Preliminary structure models were derived by application of direct methods[33] and were refined by full-matrix least-squares calculation based on F^2 for all reflections.[33] All hydrogen atoms were included in the models in calculated positions and were refined as constrained to bonding atoms.

The crystallographic data for the structures reported in this paper have been deposited with the Cambridge Crystallographic Data Center (CCDC) under http://ccdc.cam.ac.uk. Deposition numbers: CCDC 1452318 (**1a**), 1452317 (**1b**), 1452320 (**2a**), 1452319 (**2b**), 1452321 (**2c**), 1452322 (**3a**) and 1452323 (**4a**).

■ ASSOCIATED CONTENT

Supporting Information

The Supporting Information is available free of charge on the ACS Publications website at DOI: 10.1021/acs.cgd.6b00383.

Complete atom numbering schemes and ring specifications of the host molecules (PDF)

Accession Codes

CCDC 1452317−1452323 contain the supplementary crystallographic data for this paper. These data can be obtained free of charge via www.ccdc.cam.ac.uk/data_request/cif, or by emailing data_request@ccdc.cam.ac.uk, or by contacting The Cambridge Crystallographic Data Centre, 12 Union Road, Cambridge CB2 1EZ, UK; fax: +44 1223 336033.

■ AUTHOR INFORMATION

Corresponding Author

*E-mail: edwin.weber@chemie.tu-freiberg.de.

Notes

The authors declare no competing financial interest.

■ REFERENCES

(1) Vittal, J., Zaworotko, M., Tiekink, E. R. T., Eds. *Organic Crystal Engineering*; Wiley: New York, 2010.

(2) Desiraju, G. R. *Angew. Chem., Int. Ed.* **2007**, *46*, 8342−8356.

(3) Braga, D., Creponi, F., Eds. *Making Crystals by Design: Methods, Techniques and Applications*; Wiley-VCH: Weinheim, Germany, 2007.

(4) Weber, E., Ed. *Design of Organic Solids, Topics in Current Chemistry*; Springer-Verlag: Berlin, 1998; Vol. 198, pp 421−513.

(5) Herbstein, F. *Crystalline Molecular Complexes and Compounds*; Oxford University Press: Oxford, 2005; Vol. *1*, pp 421−513.

(6) Nassimbeni, L. R. In *Encyclopedia of Supramolecular Chemistry*; Atwood, J. L., Steed, J. W., Eds.; CRC Press: Boca Raton, FL, 2004; pp 696−704.

(7) Nangia, A. In *Nanoporous Materials*; Lu, G. Q., Zhao, X. S., Eds.; Series on Chemical Engineering; Imperial College Press: London, 2004; Vol. *4*, pp 165−187.

(8) *Comprehensive Supramolecular Chemistry*; MacNicol, D. D.; Toda, F.; Bishop, R., Eds.; Elsevier: Oxford, U. K., 1996; Vol. *6*.

(9) Bishop, R. In *Supramolecular Chemistry: From Molecules to Nanomaterials*; Gale, P. A., Steed, J. W., Eds.; Wiley: Chichester, U. K., 2012; Vol. *6*, pp 3033−3056.

(10) Weber, E. In *Comprehensive Supramolecular Chemistry*; MacNicol, D. D., Toda, F., Bishop, R., Eds.; Elsevier: Oxford, U. K., 1996; Vol. *6*, pp 535−592.

(11) Weber, E.; Czugler, M. In *Molecular Inclusion and Molecular Recognition − Clathrates II, Topics in Current Chemistry*; Weber, E., Ed.; Springer-Verlag: Berlin, 1988; Vol. *149*, pp 45−135.

(12) Soldatov, D. V. *J. Chem. Crystallogr.* **2006**, *36*, 747−768.

(13) Katzsch, F.; Gruber, T.; Weber, E. *Cryst. Growth Des.* **2015**, *15*, 5047−5061.

(14) Weber, E. In *Inclusion Compounds*; Atwood, J. L., Davies, J. E. D., MacNicol, D. D., Eds.; Oxford University Press: Oxford, U. K., 1991; Vol. *4*, pp 188−262.

(15) Batisai, E. F.; Nassimbeni, L. R.; Weber, E. *CrystEngComm* **2015**, *17*, 4205−4209.

(16) Weber, E.; Korkas, P. P.; Czugler, M.; Seichter, W. *Supramol. Chem.* **2004**, *16*, 217−226.

(17) Müller, T.; Hulliger, J.; Seichter, W.; Weber, E.; Weber, T.; Wübbenhorst, M. *Chem. - Eur. J.* **2000**, *6*, 54−61.

(18) Bourne, S. A.; Nassimbeni, L. R.; Niven, M. L.; Modro, A. M. *J. Inclusion Phenom. Mol. Recognit. Chem.* **1992**, *13*, 301−310.

(19) Ruffani, A.; Seichter, W.; Weber, E. *J. Inclusion Phenom. Mol. Recognit. Chem.* **2011**, *70*, 1−9.

(20) Broser, W.; Janzen, D.; Kurreck, H.; Braasch, D.; Oestreich, S.; Plato, M. *Tetrahedron* **1976**, *32*, 1819−1827.

(21) Johnson, J. R.; Grummit, O. *Org. Synth.* **1955**, Coll. Vol. *III*, 806−807.

(22) Cadogan, J. I. G.; Inward, P. W. *J. Chem. Soc.* **1962**, *0*, 4170−4178.

(23) Barber, H. J.; Slack, R. *J. Chem. Soc.* **1944**, 612−615.

(24) Sonogashira, K. In *Metal-Catalyzed Cross-Coupling Reactions*; Diederich, F., Stang, P. J., Eds.; Wiley-VCH: Weinheim, 1998.

(25) Rodriguez, J. G.; Martin-Villamil, R.; Cano, F. H.; Fonseca, I. *J. Chem. Soc., Perkin Trans. 1* **1997**, 709−714.

(26) MacBride, J. A. H.; Wade, K. *Synth. Commun.* **1996**, *26*, 2309−2316.

(27) Desiraju, G. R.; Steiner, T. *The Weak Hydrogen Bond in Chemistry and Structural Biology*; IUCR Monographs on Crystallography; Oxford University Press: New York, 1999; Vol. *9*, pp 29−121.

(28) Nishio, M.; Umezawa, Y.; Honda, K.; Tsuboyama, S.; Suezawa, H. *CrystEngComm* **2009**, *11*, 1757−1788.

(29) Bernstein, J.; Davis, R. E.; Shimoni, L.; Chang, N.-L. *Angew. Chem., Int. Ed. Engl.* **1995**, *34*, 1555−1573.

(30) Hertzsch, T.; Hulliger, J.; Weber, E.; Sozzani, P. In *Encyclopedia of Supramolecular Chemistry*; Atwood, J. L., Steed, J. W., Eds.; CRC Press: Boca Raton, FL, 2004; pp 996−1005.

(31) Eißmann, D.; Katzsch, F.; Weber, E. *Tetrahedron* **2015**, *71*, 7695−7705.

(32) Leonard, J.; Lygo, B.; Procter, G. *Praxis der Organischen Chemie*; VCH: Weinheim, 1994.

(33) Sheldrick, G. M. *Acta Crystallogr., Sect. A: Found. Crystallogr.* **2008**, *64*, 112−122.

DOI: 10.1021/acs.cgd.6b00383
Cryst. Growth Des. XXXX, XXX, XXX−XXX